

# APPLICATION OF SEQUENTIAL QUADRATIC PROGRAMMING TO MINIMIZE SMART ACTIVE FLAP ROTOR HUB LOADS

Sesi Kottapalli and Jane Leyland  
Aeromechanics Office  
NASA Ames Research Center  
Moffett Field, California  
[sesi.kottapalli@nasa.gov](mailto:sesi.kottapalli@nasa.gov) and [jane.a.leyland@nasa.gov](mailto:jane.a.leyland@nasa.gov)

In an analytical study, SMART active flap rotor hub loads have been minimized using nonlinear programming constrained optimization methodology. The recently developed NLPQLP system (Schittkowski, 2010) that employs Sequential Quadratic Programming (SQP) as its core algorithm was embedded into a driver code (NLP10x10) specifically designed to minimize active flap rotor hub loads (Leyland, 2014). Three types of practical constraints on the flap deflections have been considered. To validate the current application, two other optimization methods have been used: i) the standard, linear unconstrained method, and ii) the nonlinear Generalized Reduced Gradient (GRG) method with constraints. The new software code NLP10x10 has been systematically checked out. It has been verified that NLP10x10 is functioning as desired. The following are briefly covered in this paper: relevant optimization theory; implementation of the capability of minimizing a metric of all, or a subset, of the hub loads as well as the capability of using all, or a subset, of the flap harmonics; and finally, solutions for the SMART rotor. The eventual goal is to implement NLP10x10 in a real-time wind tunnel environment.

	Notation		
		[HL]	Hub loads column vector
A	Control amplitude vector	[HL0]	Baseline hub loads column vector, no flap deflection
A <sub>MAX</sub>	Control amplitude upper limit vector	J	Performance index, $J = g[Z(\theta)]$
A <sub>MAXΣ</sub>	Control amplitudes summation upper limit	MX, MY	Roll and pitch NP hub moments, respectively
C <sub>T</sub>	Helicopter thrust coefficient	N	Number of blades
CTHHC	Continuous-Time Higher Harmonic Control	NLP	Nonlinear programming
[CV]	Control vector, $[CV] \equiv \theta$ ; same as flap deflection vector [d] in current SMART rotor application	NLP10x10	Rotor hub loads minimization driver
[CV] <sub>max</sub>	Control vector upper limit, $[CV]_{max} \equiv \theta_{max}$	NLPQLP	Nonlinear programming system with SQP as core algorithm
[CV] <sub>min</sub>	Control vector lower limit, $[CV]_{min} \equiv \theta_{min}$	NP	N per rev
CVR	Element of the reduced control vector	SMART	Smart Material Advanced Rotor Technology
[d]	Flap deflection column vector	SQP	Sequential quadratic programming
[d*]	Optimal flap deflection column vector	[T]	T-matrix; linearly relates measurement vector to control vector
[EC]	End conditions/measurement vector, $[EC] \equiv Z$ ; same as hub loads vector [HL] in current SMART rotor application	[W]	Diagonal weighting matrix for hub loads [HL]
ECR	Element of the reduced end conditions/measurement vector	[V]	Diagonal limiting matrix for flap deflection [d]
FX, FY, FZ	Axial, side, and normal NP hub shears, respectively	Z	End conditions/measurement vector, $Z \equiv [EC]$ ; same as hub loads vector [HL] in current SMART rotor application
$g[Z(\theta)]$	General performance index function	$\alpha_s$	Rotor shaft angle
GRG	Generalized reduced gradient (method)		

$\theta$	Control vector, $\theta \equiv [\text{CV}]$ ; same as flap deflection vector $[d]$ in current SMART rotor application	$\sigma$	Rotor solidity ratio
$\theta_{\max}$	Control vector upper limit, $\theta_{\max} \equiv [\text{CV}]_{\max}$	$\phi(\theta)$	Equality constraint function
$\theta_{\min}$	Control vector lower limit, $\theta_{\min} \equiv [\text{CV}]_{\min}$	$\psi(\theta)$	Inequality constraint function
$\theta_{\text{sol}}$	Optimal solution control vector	Subscripts	
$\mu$	Rotor advance ratio	R	Reduced
		0	Previous duty cycle or reference epoch time

## Introduction

In 2008, DARPA, Boeing, the U.S. Army, and NASA completed a test of the Boeing Smart Material Advanced Rotor Technology (SMART) bearingless rotor in the USAF National Full-Scale Aerodynamics Complex 40-by 80-Foot Wind Tunnel at NASA Ames, Refs. 1-2 and Fig. 1. During the test, hub loads were successfully minimized using the continuous-time higher harmonic control (CTHHC) algorithm, Ref. 2.

Recently, a driver code specifically designed to minimize active flap rotor hub loads (NLP10x10) has been developed and used to analyze several rotorcraft control problems for which the plant was modeled by a “synthetic” randomly defined T-matrix, with the rotor hub loads also simulated by randomly defined synthetic data, Ref. 3. The NLP10x10 driver code employs the very successful recently developed NLPQLP nonlinear programming/quadratic programming system, Ref. 4. The eventual goal of the current effort is to implement NLP10x10 in a real-time wind tunnel environment.

The objectives of this paper are twofold: i) present the recently developed methodology to minimize hub loads for an active flap rotor using the constrained optimal control approach of Ref. 3; and ii) show results applicable to the full-scale SMART active flap rotor that have been used to validate the current optimization capability. Compared to Ref. 3, this paper considers more realistic simulations of an active flap rotor by using the rotorcraft comprehensive analysis CAMRAD II, Refs. 5-7, in conjunction with constrained optimal control methodology. The five-bladed bearingless SMART active flap rotor CAMRAD II model, refined and validated over the years, is used to predict the hub loads, Refs. 8-10.

An outline of this paper is as follows. First, the two other optimization methods that have been used to validate the current method are briefly described. These two other methods are: i) the standard, linear unconstrained method, and ii) the nonlinear Generalized Reduced Gradient (GRG) method with constraints. Second, the statement of the General Nonlinear Programming (NLP) Problem is given. This is followed by a brief description of the basic solution procedure NLPQLP used in this study. Next, the

formulation used in the current driver code NLP10x10 to minimize the NP hub loads of an active flap rotor is described. This is followed by a description of the implementation of the critical capability of minimizing a metric of all, or a subset, of hub loads as well as the capability of using all, or a subset, of flap harmonics as elements in the control vector. In general, the NLPQLP optimization solution procedure allows a user to specify the required constraints in a relatively straightforward manner. In NLP10x10, three types of practical constraints on the flap deflections have been implemented and a brief statement of these constraints is given in this paper. Finally, sample results for the SMART rotor active flap application and a summary of the effort to validate the current software implementation of NLP10x10 are given.

## Control Algorithms

This analytical study uses the T-matrix approach, Ref. 11. The T-matrix relates the fixed system NP hub loads to the harmonics of the trailing edge flap deflection, and is defined as follows:

$$[\text{HL}] = [\text{T}][d] + [\text{HL0}] \quad (1)$$

where  $[\text{HL0}]$  refers to the hub loads with zero (or minimal) flap deflection. The quadratic objective function  $J$  to be minimized is:

$$J = [\text{HL}]^T [\text{W}][\text{HL}] + [d]^T [\text{V}][d] \quad (2)$$

## Standard, linear unconstrained optimization

The unconstrained optimal solution  $[d^*]$  that minimizes  $J$  is:

$$[d^*] = -[\text{D}][\text{T}]^T [\text{W}][\text{HL0}] \quad (3)$$

$$\text{where } [\text{D}] = [[\text{T}]^T [\text{W}][\text{T}] + [\text{V}]]^{-1} \quad (4)$$

## GRG nonlinear optimization with constraints

In this study, the Microsoft Excel Solver version of the nonlinear algorithm GRG with constraints is used.

## Nonlinear Constrained Optimization NLP10x10

### General Nonlinear Programming (NLP) Problem

The currently addressed optimization problems are special cases of the General NLP Problem described in Refs. 3 and 12-14. The solution process involves seeking the optimal control vector  $\theta_{Sol}$  that minimizes a performance index  $J$  subject to specified constraints on the control vector  $\theta$ . For the General NLP Problem, the performance index and the constraints can in general be nonlinear. The general constrained optimization problem can be stated as follows.

Determine the vector  $\theta_{Sol}$  that solves the problem:

$$\text{Minimize } J = g[Z(\theta)] \quad (5)$$

where  $g$  can be a nonlinear function and:

$$Z = Z(\theta) = [\dots Z_q \dots]^T \quad (6)$$

$$\theta = [\dots \theta_p \dots]^T \quad (7)$$

The subscripts  $q$  and  $p$  denote the  $q$ -th and  $p$ -th elements of the  $Z$  and  $\theta$  vectors, respectively.

The problem is subject to direct constraints on the control vector  $\theta$ :

$$-\infty < \theta_{\min p} \leq \theta_p \leq \theta_{\max p} < +\infty$$

Direct constraints (8)

and general equality and inequality constraints:

$$\phi(\theta) = 0 \quad \text{Equality constraints} \quad (9)$$

$$\psi(\theta) \leq 0 \quad \text{Inequality constraints} \quad (10)$$

The vectors  $\phi$  and  $\psi$  can have different dimensions.

### NLP problem solution by NLPQLP

An investigation of various methods (Ref. 15) that can solve the general NLP problem led to the current selection of the method of Schittkowski (Ref. 4) that is partially based on related methods by Schittkowski, Powell, Stoer, and Gill (Refs. 16-22). These methods solve the general NLP problem by solving a sequence of related quadratic programming sub-problems until either convergence to the desired solution is obtained or the specified maximum number of iterations (i.e., the maximum number of quadratic programming sub-problems to be solved) is reached. This process is described in detail in Ref. 12.

One important advantage of this technique is that quadratic programming problems can be solved efficiently. A very important property of quadratic programming problems is that if the quadratic coefficient matrix in the performance index is positive definite, the problem has a unique solution which is, of course, the global solution. This means that the sequence of solutions to the quadratic programming sub-problems will converge to the global solution of the general problem in the limit, provided that the quadratic coefficient matrix in the performance index remains positive definite in the process.

The NLP algorithm described in Ref. 23 is coded in Fortran 77 and available as IMSL library routines (specifically, IMSL main driver routines DNCONF and DNCONG described in Ref. 23). This IMSL NCONF/DNCONF subroutine system, dating back to 1989, worked quite well in the research described in Refs. 12 and 15 and has proven to be quite robust and efficient in those applications. Professor Klaus Schittkowski of the University of Bayreuth, Germany, has subsequently revised and updated his Sequential Quadratic Programming (SQP) method that is part of the IMSL MATH/LIBRARY via several versions of the original code, which has resulted in performance improvements and error eliminations. This revised SQP code is available by license as the stand-alone NLPQLP code.

In the NLPQLP system, the successive quadratic programming sub-problems to be solved are formulated by using a quadratic approximation for the general NLP performance index  $J = g[Z(\theta)]$  and linear approximations for the general NLP equality and inequality constraint functions  $\phi(\theta)$  and  $\psi(\theta)$ . These approximations are obtained by a simple replacement of the  $g[Z(\theta)]$ ,  $\phi(\theta)$ , and  $\psi(\theta)$  functions with their appropriately truncated matrix Taylor series expansions. Specifically, the matrix Taylor series expansion for  $J = g[Z(\theta)]$  is truncated after the quadratic term. The quadratic coefficient of the truncated  $g[Z(\theta)]$  is its

Hessian, that is  $\partial^2 g(\theta) / \partial \theta^2$ . If the Hessian does not remain positive definite during the iteration process, the NLPQLP algorithm adjusts it so that it is positive definite in order to assure global optimality of this newly defined quadratic programming sub-problem. The matrix Taylor series expansions for the constraint functions  $\phi(\theta)$  and  $\psi(\theta)$  are truncated after their linear terms. The linear coefficients of these constraint functions are their respective gradients  $\partial \phi(\theta) / \partial \theta$  and  $\partial \psi(\theta) / \partial \theta$ . If optimality, as measured by the Kuhn-Tucker (KT) criterion at the completion of an iteration step, is not satisfied and if the specified maximum number of

iterations has not been reached, the Hessian and the constraint gradients are updated (Refs. 4 and 23); a new quadratic programming sub-problem is defined. A new iteration is then initiated starting with the last value of  $\theta$  and the newly updated Hessian and constraint gradients.

### Active flap rotor hub loads minimization, NLP10x10

The NLP10x10 solution process seeks to minimize the performance measure/index defined by the weighted squares of the selected fixed system NP rotor hub load(s). The NP hub loads that can be considered are: axial, side, and normal forces and roll and pitch moments. The process assumes that these hub loads are controllable by trailing edge flap deflections at frequencies of 2P, 3P, 4P, 5P, and 6P, individually or combined. Constraints on the individual and sum of flap deflections can be imposed as required. A linear global plant model (i.e., T-Matrix formulation) that linearly relates the measurement vector (sine and cosine components of the hub loads) to the control vector (sine and cosine components of the flap deflections) is assumed. This model is widely used in rotorcraft aeromechanical behavior studies.

In the description that follows, an attempt has been made to make the notation consistent with the variable names used in the Fortran code NLP10x10 in order to facilitate easier understanding of the code. The most general model that is addressed in this research and treated by the NLP10x10 system assumes the following:

i) The general end conditions vector [EC] is a (10x1) vector composed of the sine and cosine components of the NP axial, side, and normal hub shears and the roll and pitch hub moments.

ii) The general control vector [CV] is a (10x1) vector composed of five harmonics of the flap deflection, that is, the sine and cosine components of the 2P, 3P, 4P, 5P, and 6P flap deflection angles. The corresponding T-matrix is a (10x10) matrix. The general model relates the general end conditions vector [EC] to the general control vector [CV] according to the equation:

$$[EC] = [T][CV] + [EC]_0 \quad (11)$$

where

$[EC]_0$  is [EC] defined during a previous duty cycle or a reference epoch time

$EC_i$  and  $EC0_i$  are the  $i$ -th elements of [EC] and  $[EC]_0$ , respectively and

$CV_j$  is the  $j$ -th element of [CV].

Let FX, FY, and FZ be the axial, side, and normal NP hub forces and MX and MY be the NP hub roll and pitch moments, respectively. Then let the suffixes S and C denote the sine and cosine components of the NP hub forces and the NP hub moments, respectively (e.g., FXS and FXC denote the sine and cosine components of FX, respectively). Also, let d2, d3, d4, d5, d6 denote the respective 2P, 3P, 4P, 5P, 6P harmonics of the flap deflection angles. As in the case of the hub loads, the suffixes S and C denote the sine and cosine components of the harmonics of the flap deflection angles (e.g., d2S and d2C denote the sine and cosine components of the 2P flap deflection angle, respectively). The general [EC] and [CV] vectors then have the following forms as shown in Eq. (12) below.

This general representation includes all hub load components and separately, all flap deflections. A major

$$\left. \begin{aligned} [EC] &= \begin{bmatrix} EC_1 \\ EC_2 \\ EC_3 \\ EC_4 \\ EC_5 \\ EC_6 \\ EC_7 \\ EC_8 \\ EC_9 \\ EC_{10} \end{bmatrix} = \begin{bmatrix} FXS \\ FXC \\ FYS \\ FYC \\ FZS \\ FZC \\ MXS \\ MXC \\ MYS \\ MYC \end{bmatrix} \\ &\text{and} \\ [CV] &= \begin{bmatrix} CV_1 \\ CV_2 \\ CV_3 \\ CV_4 \\ CV_5 \\ CV_6 \\ CV_7 \\ CV_8 \\ CV_9 \\ CV_{10} \end{bmatrix} = \begin{bmatrix} d2S \\ d2C \\ d3S \\ d3C \\ d4S \\ d4C \\ d5S \\ d5C \\ d6S \\ d6C \end{bmatrix} \end{aligned} \right\} \quad (12)$$

and critical feature is the capability to allow for all 10 hub load components to be actively considered or a specified selected subset of hub load components (e.g., only FX, or only FX and FY, etc.) to be actively considered. All 10 flap deflection components can be actively considered or a specified selected subset of these flap deflection components can be actively considered. For these purposes, NLP10x10 provides options to reduce the number of elements in the general model, which can result in a reduced model. Sine and cosine pairs of elements of either or both the general end conditions (10x1) vector  $[EC]$  and/or the general control vector (10x1) vector  $[CV]$  can be eliminated to define a reduced model. In these cases, the T-matrix size is reduced by eliminating the appropriate rows and/or columns to define a reduced matrix,  $[T]_R$ . This reduced model relates the reduced end conditions vector  $[EC]_R$  to the reduced control vector  $[CV]_R$  according to:

$$[EC]_R = [T]_R [CV]_R + [EC]_{OR} \quad (13)$$

where

$[T]_R$  is the correspondingly reduced T-matrix and

$[EC]_{OR}$  is the reduced  $[EC]_R$  vector defined during a previous duty cycle.

The NLP10x10 system needs the following three elements of information as inputs: 1) the T-matrix; 2) the actual previous cycle control vector  $[CV]_0$ ; and 3) the actual previous cycle measurement vector  $[EC]_0$ . Two options are currently provided in the NLP10x10 system to define these three elements. These options are: 1) Synthetically define the above three elements using a uniformly distributed random function to generate these elements; and 2) Input actual test data or analytically simulated data to define these three elements. The synthesis option (i.e., Option 1) has been successfully used for check out prior to using actual test data. In the current full-scale SMART rotor application, analytically simulated data (i.e., Option 2) obtained using the CAMRAD II model of the SMART rotor (Refs. 8-10) was used to define these three elements.

### Implementation of model dimension reduction

The core of the driver code NLP10x10 consists of logic that ultimately provides the user with the capability to specify the NP hub load(s) to be minimized and the control to be used, i.e. the flap deflection harmonic(s) to be used in the minimization process. Within the driver code NLP10x10, the first major step pertaining to the specific problem of interest is to define: i) the user specified NP hub load couples (sine and cosine pairs) to

be minimized; these couples are the end conditions to be considered for the specific problem; and ii) the user specified control, i.e. the flap deflection harmonics. Only an outline of the model reduction process is given here. In the context of the above considerations, let:

$M_{EC}$  denote the total number of selected end conditions NP hub load couples (sine and cosine pairs of the specified hub load elements); these end conditions are selected from the general end condition vector  $[EC]$  to comprise the reduced vectors  $[EC]_R$  and  $[EC]_{OR}$ , respectively.

$N_{CV}$  denote the total number of selected control flap deflection harmonics (sine and cosine pairs) from the general control vector  $[CV]$  to comprise the reduced vector  $[CV]_R$ .

$HEC_i$  denote a preselected index, internal to NLP10x10, associated with the user specified NP hub loads couple, where  $i$  can take on values 1, 2, ..., 5.

$HCV_j$  denote a preselected index, internal to NLP10x10, associated with the user specified flap deflection harmonic, where  $j$  can take on values 1, 2, ..., 5.

Then the elements of  $[EC]_R$  (and correspondingly of  $[EC]_{OR}$ ) are:

$$ECR_i = EC_k \text{ for } i = 1, 2, 3, \dots, 2M_{EC} \text{ where } M_{EC} \leq 5 \quad (14)$$

and where the subscript  $k$  in  $EC_k$  is defined as:

$$k = \begin{cases} 2HEC_i - 1 & \text{if } i \text{ is odd} \\ 2HEC_i & \text{if } i \text{ is even} \end{cases} \quad (15)$$

The elements of  $[CV]_R$  are defined similarly:

$$CVR_l = CV_l \text{ for } l = 1, 2, 3, \dots, 2N_{CV} \text{ where } N_{CV} \leq 5 \quad (16)$$

and where the subscript  $l$  in  $CV_l$  is defined as:

$$l = \begin{cases} 2HCV_j - 1 & \text{if } j \text{ is odd} \\ 2HCV_j & \text{if } j \text{ is even} \end{cases} \quad (17)$$

The corresponding reduced T-matrix  $[T]_R$  is defined by eliminating the rows and columns from  $[T]$  that correspond to the elements eliminated from  $[EC]$ ,  $[EC]_0$ , and  $[CV]$  when constructing  $[EC]_R$ ,  $[EC]_{OR}$ , and  $[CV]_R$ , respectively.



An example of model dimension reduction is shown below where only the in-plane hub shears (i.e., the X and Y components) and a single harmonic (4P) of the flap deflection are considered. In this case, only the FX and FY components of the hub loads define  $[EC]_R$  and  $[EC]_{0R}$  and only the 4P flap deflection angle defines  $[CV]_R$ . In this case  $M_{EC}=2$ ;  $N_{CV}=1$ ;  $HEC_1=1$  and  $HEC_2=2$ ;  $HCV_1=3$ , and the corresponding reduced vector forms are:

$$\left. \begin{aligned} [EC]_R &= \begin{bmatrix} ECR_1 \\ ECR_2 \\ ECR_3 \\ ECR_4 \end{bmatrix} = \begin{bmatrix} FXS \\ FXC \\ FYS \\ FYC \end{bmatrix} \\ &\text{and} \\ [EC]_{0R} &= \begin{bmatrix} EC0R_1 \\ EC0R_2 \\ EC0R_3 \\ EC0R_4 \end{bmatrix} = \begin{bmatrix} FXS0 \\ FXC0 \\ FYS0 \\ FYC0 \end{bmatrix} \\ &\text{and} \\ [CV]_R &= \begin{bmatrix} CVR_1 \\ CVR_2 \end{bmatrix} = \begin{bmatrix} CV_5 \\ CV_6 \end{bmatrix} \\ &= \begin{bmatrix} d4S \\ d4C \end{bmatrix} \end{aligned} \right\} (18)$$

where

$ECR_i$  and  $EC0R_i$  are the  $i$ -th elements of  $[EC]_R$  and  $[EC]_{0R}$  vectors, respectively and

$CVR_j$  is the  $j$ -th element of  $[CV]_R$ .

### NLP problem with constraints on flap deflection

This problem is a special case of the general NLP problem outlined previously. The optimization problem seeks to minimize the performance index  $J$  consisting of selected NP hub loads and subject to specified constraints on the flap deflection. The actual SMART rotor, Ref. 1,

has hard limits for the maximum flap deflection. Any combination of the following three types of constraints is currently available in NLP10x10: i) constraints imposed directly on each flap deflection harmonic, i.e. on each element  $CVR_j$  of the reduced vector  $[CV]_R$ ; ii) constraints imposed on selected flap deflection amplitudes, i.e. on elements of  $[CV]_R$ ; and iii) a constraint imposed on the summation of selected amplitudes of the flap deflection. Specifically the minimization problem considered in this study is:

$$\text{Minimize } J = \sum_{i=1}^{2M_{EC}} W_i (ECR_i)^2 \quad (19)$$

where  $W_i$  is a specified weighting coefficient.

The problem is subject to one of the following three types of constraints:

i) *Direct control element constraints:*

$$-\infty < CV_{\min j} \leq CV_j \leq CV_{\max j} < +\infty$$

$$\text{where } j = 1, 2, 3, \dots, 2N_{CV} \quad (20)$$

ii) *Control amplitudes constraints:*

$$A_q = \sqrt{CV_{2q-1}^2 + CV_{2q}^2} \leq A_{\max q} \quad (21)$$

where the subscript  $q$  is determined by user specified flap harmonic(s) and preselected index number(s) internal to NLP10x10.

iii) *Control amplitude summation constraint:*

$$\sum_p A_p \leq A_{\max \Sigma} \quad (22)$$

where the subscript  $p$  is determined by user specified flap harmonic(s) and preselected index number(s) internal to NLP10x10.

### Results

The five-bladed bearingless SMART active flap rotor CAMRAD II model was used to predict the hub loads, Refs. 8-10. The selected operating condition is one of the operating conditions in the Vibration Control part of the SMART rotor wind tunnel test (Ref. 1):  $\mu=0.3$ ,  $C_T/\sigma=0.075$ ,  $\alpha_s=-9.1^\circ$ . The T-matrix has been assembled

using ten CAMRAD II runs, each with 1° trailing edge flap amplitude; for example, a run with 1° 3P cosine flap amplitude has all other flap components close to zero.

As noted earlier, the standard, linear unconstrained method has been used first to get optimal flap deflections for a number of specified cases, and then for validation purposes NLP10x10 was used to get optimal solutions for the same cases. For the constrained cases considered in this study, optimal solutions have been obtained using both NLP10x10 and GRG. The NLP10x10 validation effort is discussed in the next section with the linear unconstrained solution results presented below.

### Linear unconstrained solution results

An initial estimate of the optimal solution  $[d^*]$  is obtained from Eq. (1) by setting its left side to zero, giving:

$$[d^*] = - [T]^{-1} [HL0] \quad (23)$$

This optimal flap deflection is shown in Fig. 2. The maximum flap deflection is less than 0.8° and includes all 5 harmonic flap inputs. For a quadratic performance index  $J$  with all 10 hub load components equally weighted, the  $[d^*]$  from Fig. 2 results in 12% reduction in  $J$ . The baseline and optimal hub loads are shown in Table 1; all hub loads except MYC (cosine component of the pitch moment) are reduced.

Next, the 5P hub shears are considered individually. A single harmonic flap input is considered. Optimal solutions using  $[d^*]$  from Eq. (3) have been obtained for the following three scenarios: i) Minimize normal shear FZ; ii) Minimize axial shear FX; and iii) Minimize side shear FY. The frequency of the single harmonic input has been varied from 2P to 6P (5 separate optimal inputs for each shear; total 15 CAMRAD II cases, each with one optimal input). Since the T-matrix was calculated using 1° flap amplitude, the current optimal flap amplitudes are kept reasonable by adjusting the diagonal limiting matrix  $[V]$ , and the resulting amplitude range turns out to be 0.33° to 1.44°.

Figures 3a-3c show the resulting minimizations for FZ, FX, and FY, respectively. Each figure shows the shears, moments, and three indexes, defined as follows. The first two indexes are based on equally weighted shears and separately, moments, and the third is a total index that includes both shear and moment components (equally weighted). The best reductions are listed as follows:

- i) FZ minimization, Fig. 3a: 4P input reduces FZ by 90%. A 5P input is also effective. The effectiveness of the 4P and 5P inputs is consistent with the SMART rotor test results, Ref. 1.

- ii) FX minimization, Fig. 3b: 5P input reduces FX by 37%.

- iii) FY minimization, Fig. 3c: 4P input reduces FY by 50%.

Overall, the three best reductions in the total index with all hub loads equally weighted are as follows:

<u>Reduction in total index</u>	<u>Hub shear minimized</u>	<u>Active harmonic</u>
27%	FZ	4P
24%	FX	5P
20%	FY	4P

The bottom charts in Figs. 3a-3c show the actual indexes. The current reductions in hub shears are encouraging. The linear unconstrained solution design space allows for solutions with single harmonic inputs that give better reductions compared to a solution using all 5 harmonics. The linear unconstrained method does not guarantee a globally optimum solution.

### NLP10x10 validation

As noted in a previous section, NLP10x10 including NLPQLP and associated subroutines were first installed on a mainframe (operating system OpenVMS, Fortran 77) and code debugging and fine-tuning of the algorithm was done on this mainframe. In order to prepare for an eventual wind tunnel installation, the OpenVMS code was ported to a Mac desktop (OS 10.6, gfortran). Compatibility issues were encountered and a significant amount of time and effort was expended in resolving these issues. Currently, all compatibility issues have been sorted out and NLP10x10 can be run on both systems.

The current NLP10x10 software with NLPQLP as its core algorithm has been validated in the following manner.

### Unconstrained cases

A major and critical step is the development and verification of the capability to allow for all 10 hub load components to be actively considered at one time or a specified, selected set of hub load components (e.g., only FX, or only FX and FY, etc.) to be actively considered. An additional complexity is the development and verification of the capability to allow the flap deflection vector to be fully populated or partially populated depending on the specified control harmonic(s) under active consideration. Over 35 cases (Table 2) have been formulated and used to successfully validate these capabilities. Finally, it has been confirmed that the

NLP10x10 optimal solutions are the same as or very close to all of the solutions obtained from the standard linear method (Table 3).

### Constrained cases

For the unconstrained test cases studied so far, two of the cases have resulted in relatively large optimal flap deflections (Cases 20 and 25, Tables 2-3). NLP10x10 has been successfully run with constraints in order to limit the flap amplitude. Several cases have been considered with a specified, wide limiting amplitude range ( $0.1^\circ$  to  $9^\circ$ ). Individual test cases have been run with the following amplitude limits:  $0.1^\circ$ ,  $0.3^\circ$ ,  $0.6^\circ$ , and  $1^\circ$  to  $9^\circ$  in steps of  $1^\circ$ . It has been confirmed that the resulting constrained NLP10x10 and GRG optimal solutions are the same or very close to each other (Table 4).

### Sensitivity to starting conditions

The sensitivity of the NLP10x10 optimal solutions to the initial starting conditions has been studied by starting with both best guess starting conditions based on the standard linear method (that is,  $[d_o]=[d^*]$  from Eq. 3) and zero initial conditions ( $[d_o]=[0]$ ). The results show that for the current application the NLP10x10 method is relatively insensitive to the starting conditions. A preliminary observation is that there is some increase in the number of iterations required for convergence (Tables 5-6). This topic will have to be eventually revisited for a more comprehensive evaluation during the actual use of the method in a real-time wind tunnel environment.

Thus, it appears that the current software is functioning as desired.

### Conclusions

A new software code NLP10x10 that employs the nonlinear optimization algorithm NLPQLP was developed with the purpose of minimizing active flap rotor hub loads in a real-time wind tunnel environment. Full-scale SMART active flap rotor hub loads were analytically minimized using the current nonlinear programming constrained optimization methodology. It was verified that the new code is functioning as desired. Details on this analytical effort were presented.

### References

1. Straub, F. K., Anand, V. R., Birchette, T. S., and Lau, B. H., "Wind Tunnel Test of the SMART Active Flap Rotor," American Helicopter Society 65th Annual Forum Proceedings, Grapevine, TX, May 27-29, 2009.
2. Hall, S. R., Anand, V. R., Straub, F. K., and Lau, B.H., "Active Flap Control of the SMART Rotor for Vibration Reduction," American Helicopter Society 65th Annual Forum Proceedings, Grapevine, TX, May 27-29, 2009.
3. Leyland, J. A., "Use of the NLPQLP Sequential Programming Algorithm to Solve Rotorcraft Aeromechanical Constrained Optimisation Problems, Volume 1: Theory and Methodology," NASA TM-2014-216632.
4. Schittkowski, K., "NLPQLP: a FORTRAN Implementation of a Sequential Quadratic Programming Algorithm with Distributed and Non-Monotone Line Search – User's Guide," Version 3.1, Department of Computer Science, University of Bayreuth, Germany, February 2010.
5. Johnson, W., "CAMRAD II, Comprehensive Analytical Model of Rotorcraft Aerodynamics and Dynamics," Johnson Aeronautics, Palo Alto, California, 1992-1999.
6. Johnson, W., "Technology Drivers in the Development of CAMRAD II," American Helicopter Society, American Helicopter Society Aeromechanics Specialists Conference, San Francisco, CA, January 19-21, 1994.
7. Johnson, W., "A General Free Wake Geometry Calculation for Wings and Rotors," American Helicopter Society 51st Annual Forum Proceedings, Ft. Worth, TX, May 9-11, 1995.
8. Kottapalli, S. and Straub, F.K., "Correlation of SMART Active Flap Rotor Loads," American Helicopter Society 65th Annual Forum Proceedings, Grapevine, TX, May 27-29, 2009.
9. Kottapalli, S., "Low-Speed and High-Speed Correlation of SMART Active Flap Rotor Loads," American Helicopter Society Aeromechanics Specialists' Conference, San Francisco, CA, January 20-22, 2010.
10. Kottapalli, S., "Enhanced Correlation of SMART Active Flap Rotor Loads," American Institute of Aeronautics and Astronautics 52nd AIAA/ASME/ASCE/AHS/ASC Structures, Structural Dynamics, and Materials Conference, Denver, CO, April 4-7, 2011, AIAA 2011-1874.
11. Johnson, W., "Self-Tuning Regulators for Multicyclic Control of Helicopter Vibration," NASA TP 1996, March 1982.



12. Leyland, J. A., "A Closed-Loop Optimal Neural-Network Controller to Optimise Rotorcraft Aeromechanical Behaviour, Volume 1, Theory and Methodology" NASA TM-2001-209622, March 2001.
13. Leyland, J. A., "A General Regularisation Functional to Enhance the Update Convergence of a Neural-Network Rotorcraft Behaviour Model, Volume 1, Theory and Methodology" NASA TM-2002-211843, October 2002.
14. Leyland, J. A., "Experimentation with the Regularised Optimal Neural-Network Controller (RONNC) System Applied to Rotorcraft Aeromechanical Problems, Volume 1, Theory and Methodology", to be published.
15. Leyland, J. A., "A Higher Harmonic Optimal Controller to Optimise Rotorcraft Aeromechanical Behaviour," NASA TM 110390, March 1996.
16. Gill, P.E., W. Murray, M. A. Saunders, and M. H. Wright, "Model Building and Practical Aspects of Non-Linear Programming", *Computational Mathematical Programming*, edited by K. Schittkowski, NATO ASI Series, 15, Springer-Verlag, Berlin, Germany, 1985.
17. Powell, M. J. D., "A Fast Algorithm for Non-linearly Constrained Optimization Calculations," *Numerical Analysis Proceedings*, Dundee, 1977.
18. Powell, M. J. D., "A Fast Algorithm for Non-linearly Constrained Optimization Calculations," *Lecture Notes in Economics and Mathematics*, **630**, Springer-Verlag, Berlin, Germany, pp. 144-157, 1978.
19. Schittkowski, K., "Non-linear Programming Codes," *Lecture Notes in Economics and Mathematics*, 183, Springer-Verlag, Berlin, Germany, 1980.
20. Schittkowski, K., "On the Convergence of a Sequential Quadratic Programming Method with an Augmented Lagrangian Line Search Function," *Mathematik Operationsforschung und Statistik, Serie Optimization*, 14, pp. 197-216, 1983.
21. Schittkowski, K., "NLPQL: a FORTRAN Subroutine solving Constrained Non-linear Programming Problems," edited by Clyde L. Monma, *Annals of Operations Research*, 5, pp. 485-500, 1986.
22. Stoer, J., "Principles of Sequential Quadratic Programming Methods in Solving Non-Linear Problems," *Computational Mathematical Programming*, edited by K. Schittkowski, NATO ASI Series, 15, Springer-Verlag, Berlin, Germany, 1985.
23. IMSL MATH/LIBRARY User's Manual, "FORTRAN Subroutines for Mathematical Applications, Volume 3, Chapter 8: Nonlinearly Constrained Minimization Using Finite Difference Gradients," Version 1.1, MALB-USM-UNBND-EN8901-1.1, pp. 895-902, January 1989.

**Table 1. Baseline and minimized hub loads from initial estimate of optimal solution, linear unconstrained method.**

<b>Hub load</b>	<b>Baseline, lb, ft-lb</b>	<b>From optimal solution Eq. 23, lb, ft-lb</b>
FXC	75.6	75.3
FYC	80.7	72.0
FZC	77.7	67.7
MXC	31.4	23.4
MYC	12.2	24.1
FXS	-95.5	-82.8
FYS	84.9	81.7
FZS	-65.8	-42.3
MXS	-37.3	-32.2
MYS	43.6	29.7

**Table 2. NLP10x10 validation cases (unconstrained).**

<b>Case</b>	<b>Hub load (sine and cosine)</b>	<b>Control inputs (sine and cosine)</b>
1	FX, FY, FZ, MX, MY	2P, 3P, 4P, 5P, 6P
2	FX, FY, FZ, MX, MY	3P, 4P, 5P
3 to 7	FX, FY, FZ, MX, MY	Single harmonic, 2P to 6P
8 to 12	FX, FY, FZ	Single harmonic, 2P to 6P
13 to 17	MX, MY	Single harmonic, 2P to 6P
18 to 22	FX	Single harmonic, 2P to 6P
23 to 27	FY	Single harmonic, 2P to 6P
28 to 32	FZ	Single harmonic, 2P to 6P
33 to 37	FX, FY	Single harmonic, 2P to 6P

**Table 3. Comparison of standard (Eq. 3) and NLP10x10 optimal flap deflections (unconstrained).**

Case	Hub load(s) minimized	Active harmonic(s)	cosine, deg		sine, deg	
			Std.	NLP10x10	Std.	NLP10x10
1	FX, FY, FZ, MX, MY	2P	-0.33	-0.33	-0.16	-0.16
1	"	3P	0.23	0.23	0.08	0.08
1	"	4P	0.00	0.00	-0.16	-0.16
1	"	5P	-0.12	-0.12	-0.19	-0.19
1	"	6P	-0.17	-0.17	-0.02	-0.02
2	FX, FY, FZ, MX, MY	3P	-1.02	-1.03	-0.55	-0.55
2	"	4P	-0.40	-0.40	0.49	0.50
2	"	5P	0.09	0.09	0.19	0.19
3	FX, FY, FZ, MX, MY	2P	-0.49	-0.50	-0.37	-0.38
4	"	3P	-0.54	-0.55	-0.62	-0.63
5	"	4P	-0.61	-0.65	-0.02	-0.01
6	"	5P	-0.21	-0.22	-0.36	-0.38
7	"	6P	-0.29	-0.31	-0.41	-0.47
8	FX, FY, FZ	2P	-0.46	-0.47	-0.39	-0.39
9	"	3P	-0.81	-0.81	-0.43	-0.44
10	"	4P	-0.85	-0.90	0.25	0.29
11	"	5P	-0.19	-0.19	-0.39	-0.40
12	"	6P	-0.48	-0.51	-0.57	-0.60
13	MX, MY	2P	-0.95	-0.95	-0.16	-0.15
14	"	3P	-0.33	-0.34	-1.04	-1.04
15	"	4P	-0.30	-0.30	-0.18	-0.18
16	"	5P	-0.37	-0.38	-0.19	-0.19
17	"	6P	-0.23	-0.23	-0.12	-0.12
18	FX	2P	-0.51	-0.51	-0.30	-0.30
19	"	3P	-1.55	-1.55	0.09	0.09
20	"	4P	4.05	4.49	-8.05	-8.76
21	"	5P	0.02	0.02	-0.69	-0.69
22	"	6P	-1.12	-1.12	-0.46	-0.46
23	FY	2P	-0.44	-0.44	-0.38	-0.38
24	"	3P	-1.10	-1.10	-0.23	-0.23
25	"	4P	-3.39	-3.48	3.89	4.03
26	"	5P	0.34	0.34	-0.90	-0.90
27	"	6P	-0.44	-0.44	-1.06	-1.06
28	FZ	2P	-0.45	-0.45	-0.64	-0.64
29	"	3P	-0.37	-0.37	-0.97	-0.97
30	"	4P	-0.80	-0.80	0.60	0.60
31	"	5P	-0.17	-0.17	-0.29	-0.29
32	"	6P	1.15	1.15	-0.81	-0.82
33	FX, FY	2P	-0.48	-0.48	-0.33	-0.33
34	"	3P	-1.28	-1.28	-0.10	-0.09
35	"	4P	-1.25	-1.31	0.62	0.68
36	"	5P	0.13	0.13	-0.76	-0.76
37	"	6P	-0.65	-0.66	-0.70	-0.71

**Table 4. Comparison of GRG and NLP10x10 optimal flap deflections (constrained).**

Hub shear minimized	Active harmonic	Constraint deg	<u>cosine, deg</u>		<u>sine, deg</u>	
			GRG	NLP10x10	GRG	NLP10x10
FX	4P	None	4.49	4.49	-8.76	-8.76
"	"	9.0	4.04	4.04	-8.04	-8.04
"	"	8.0	3.52	3.52	-7.19	-7.19
"	"	7.0	2.99	2.99	-6.33	-6.33
"	"	6.0	2.47	2.47	-5.47	-5.47
"	"	5.0	1.94	1.94	-4.61	-4.61
"	"	4.0	1.41	1.41	-3.74	-3.74
"	"	3.0	0.87	0.87	-2.87	-2.87
"	"	2.0	0.32	0.32	-1.97	-1.97
"	"	1.0	-0.30	-0.30	-0.96	-0.96
"	"	0.6	-0.50	-0.50	-0.33	-0.33
"	"	0.3	-0.25	-0.25	-0.16	-0.16
"	"	0.1	-0.08	-0.08	-0.05	-0.05
FY	4P	None	-3.48	-3.48	4.03	4.03
"	"	5.0	-3.30	-3.30	3.76	3.76
"	"	4.0	-2.75	-2.75	2.91	2.91
"	"	3.0	-2.19	-2.19	2.05	2.05
"	"	2.0	-1.62	-1.62	1.17	1.17
"	"	1.0	-0.98	-0.98	0.19	0.19
"	"	0.6	-0.52	-0.52	-0.30	-0.30
"	"	0.3	-0.25	-0.25	-0.16	-0.16
"	"	0.1	-0.08	-0.08	-0.05	-0.05

**Table 5. Comparison of number of iterations for best guess start and zero initial conditions (unconstrained) using NLP10x10.**

Case	Hub load(s) minimized	Active harmonic(s)	Best guess start	Zero initial conditions
1	FX, FY, FZ, MX, MY	2P, 3P, 4P, 5P, 6P	14	19
2	FX, FY, FZ, MX, MY	3P, 4P, 5P	13	13
3	FX, FY, FZ, MX, MY	2P	5	9
4	"	3P	7	8
5	"	4P	9	9
6	"	5P	7	8
7	"	6P	8	8
8	FX, FY, FZ	2P	5	8
9	"	3P	9	8
10	"	4P	9	8
11	"	5P	6	8
12	"	6P	8	7
13	MX, MY	2P	9	7
14	"	3P	6	8
15	"	4P	7	6
16	"	5P	6	7
17	"	6P	7	7
18	FX	2P	6	8
19	"	3P	7	8
20	"	4P	6	7
21	"	5P	6	8
22	"	6P	9	9
23	FY	2P	6	7
24	"	3P	7	8
25	"	4P	6	6
26	"	5P	6	7
27	"	6P	7	7
28	FZ	2P	8	10
29	"	3P	6	8
30	"	4P	8	8
31	"	5P	7	6
32	"	6P	10	10
33	FX, FY	2P	5	8
34	"	3P	7	8
35	"	4P	8	6
36	"	5P	6	8
37	"	6P	7	7



**Table 6. Comparison of number of iterations for best guess start and zero initial conditions (constrained) using NLP10x10.**

<b>Hub shear minimized</b>	<b>Active harmonic</b>	<b>Constraint deg</b>	<b>Best guess start</b>	<b>Zero initial conditions</b>
FX	4P	None	6	7
"	"	9.0	7	7
"	"	8.0	7	7
"	"	7.0	7	7
"	"	6.0	6	6
"	"	5.0	6	6
"	"	4.0	6	6
"	"	3.0	6	6
"	"	2.0	6	6
"	"	1.0	7	7
"	"	0.6	10	10
"	"	0.3	9	9
"	"	0.1	10	13
FY	4P	None	6	6
"	"	5.0	7	6
"	"	4.0	6	6
"	"	3.0	6	6
"	"	2.0	7	7
"	"	1.0	7	7
"	"	0.6	10	10
"	"	0.3	9	9
"	"	0.1	13	12

**Fig. 1. Boeing SMART active flap rotor installed in USAF National Full-Scale Aerodynamics Complex 40- by 80-Foot Wind Tunnel, Refs. 1-2.**



**Fig. 2. Initial estimate of optimal flap deflection using the linear unconstrained method, Eq. (23),  $\mu=0.3$ ,  $C_T/\sigma=0.075$ ,  $\alpha_s=-9.1^\circ$ .**

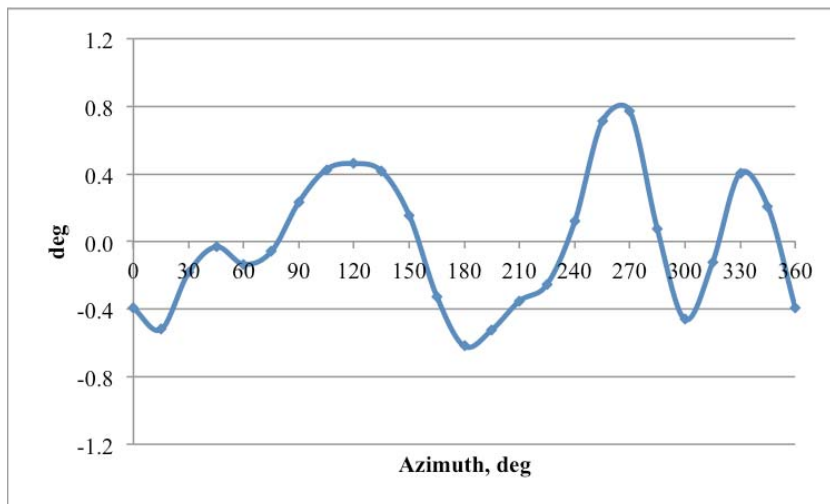


**Fig. 3a. SMART rotor FZ (normal) hub shear minimization using single harmonic flap input (2P-6P),  $\mu=0.3$ ,  $C_T/\sigma=0.075$ ,  $\alpha_s=-9.1^\circ$ .**

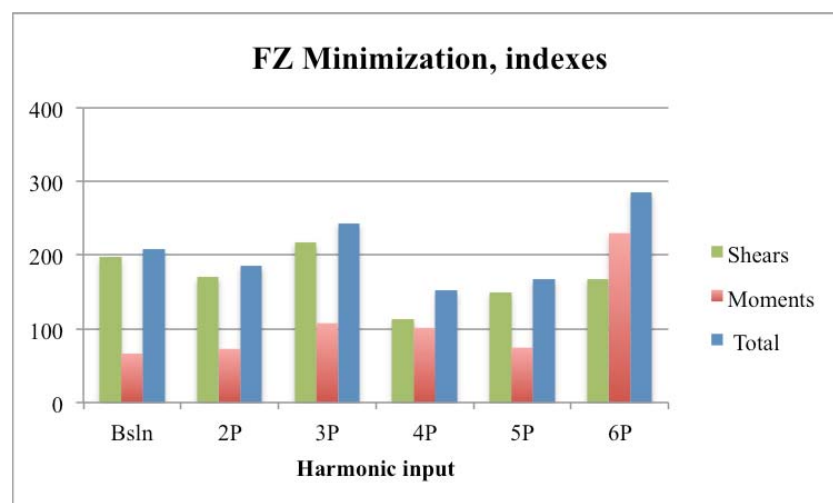
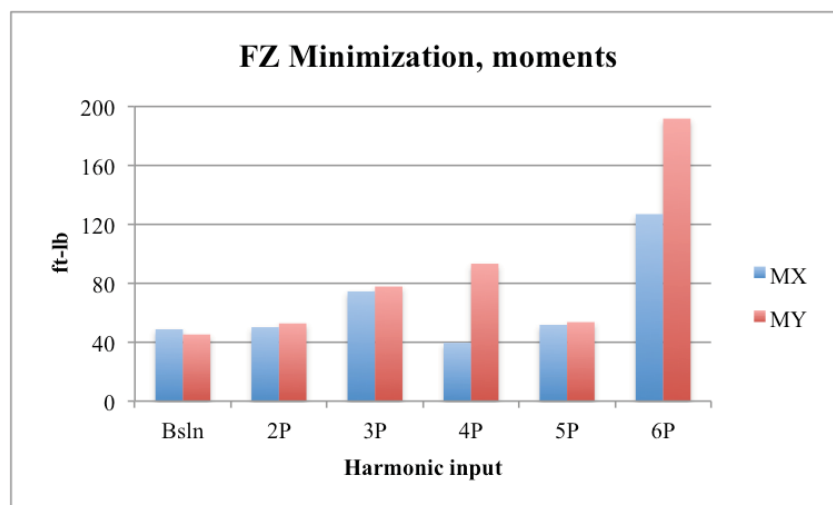
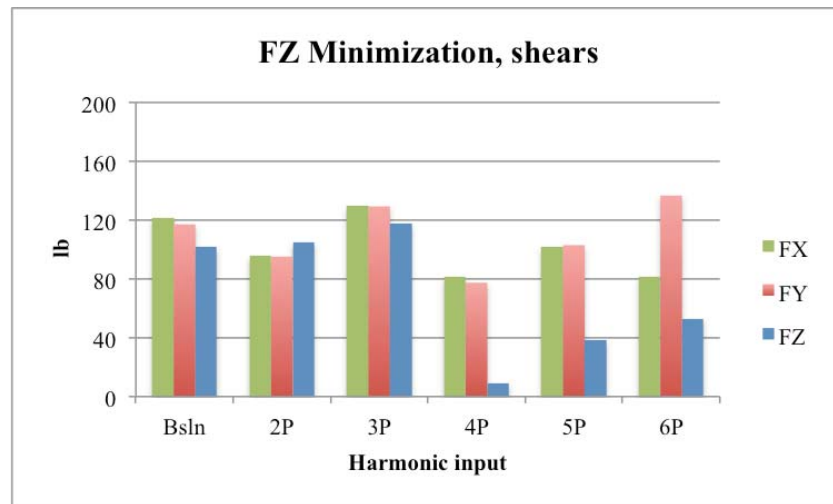


**Fig. 3b. SMART rotor FX (axial) hub shear minimization using single harmonic flap input (2P-6P),  $\mu=0.3$ ,  $C_T/\sigma=0.075$ ,  $\alpha_s=-9.1^\circ$ .**

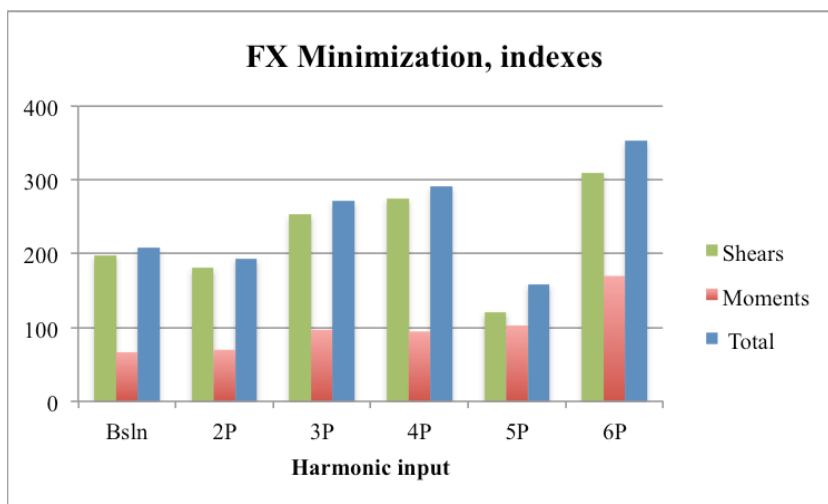
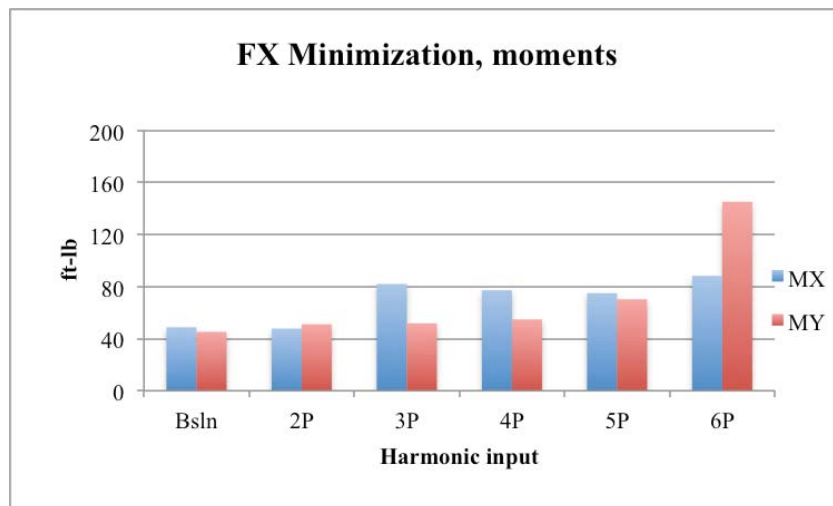
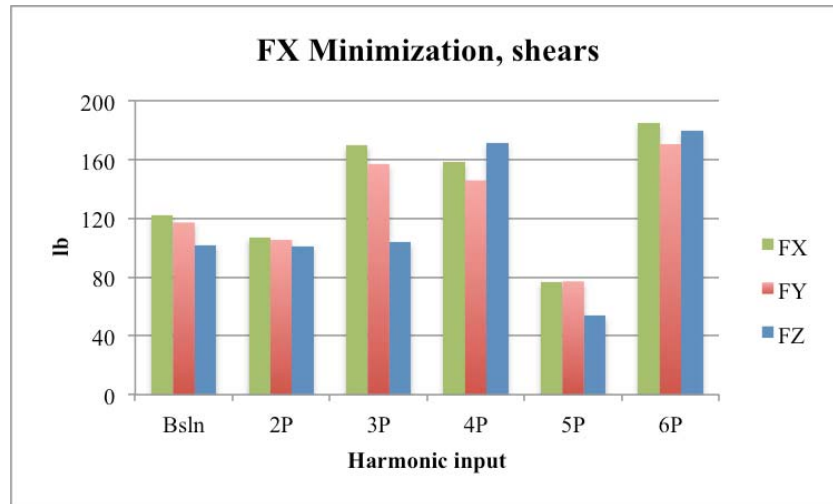


**Fig. 3c. SMART rotor FY (side) hub shear minimization using single harmonic flap input (2P-6P),  $\mu=0.3$ ,  $C_T/\sigma=0.075$ ,  $\alpha_s=-9.1^\circ$ .**

